# High-order moments of spin-orbit energy in a multielectron configuration

Xieyu Na and M. Poirier*

*Laboratoire "Interactions, Dynamiques et Lasers", UMR 9222, CEA-CNRS-Université Paris-Saclay, Centre d'Études de Saclay, F91191 Gif-sur-Yvette, Cedex, France*

(Received 4 May 2016; revised manuscript received 17 June 2016; published 25 July 2016)

In order to analyze the energy-level distribution in complex ions such as those found in warm dense plasmas, this paper provides values for high-order moments of the spin-orbit energy in a multielectron configuration. Using second-quantization results and standard angular algebra or fully analytical expressions, explicit values are given for moments up to 10th order for the spin-orbit energy. Two analytical methods are proposed, using the uncoupled or coupled orbital and spin angular momenta. The case of multiple open subshells is considered with the help of cumulants. The proposed expressions for spin-orbit energy moments are compared to numerical computations from Cowan's code and agree with them. The convergence of the Gram-Charlier expansion involving these spin-orbit moments is analyzed. While a spectrum with infinitely thin components cannot be adequately represented by such an expansion, a suitable convolution procedure ensures the convergence of the Gram-Charlier series provided high-order terms are accounted for. A corrected analytical formula for the third-order moment involving both spin-orbit and electron-electron interactions turns out to be in fair agreement with Cowan's numerical computations.

DOI: 10.1103/PhysRevE.94.013206

## I. INTRODUCTION

The spectral properties of warm dense plasmas such as those studied in stellar atmospheres, facilities for fusion by inertial confinement, or laser-plasmas experiments may require two kinds of theoretical interpretation. On the one hand, the detailed or fine-structure accounting is based on the determination of all eigenvalues by diagonalizing the Hamiltonian usually inside a given set of configurations. On the other hand, the statistical approach relies on the characterization of emission or absorption structures by few global quantities such as the average energies, variances, and possibly moments of higher order. A wide literature has been developed on the latter approach since the noteworthy papers by Bauche *et al.* [1,2], allowing one to get approximate values for the number of levels in a configuration, estimate the number of lines in a transition array, or obtain the main parameters defining the shape of such a transition array. Within the framework of statistical spectroscopy, one may also analyze the energy distribution of levels in a configuration $\mathscr{C}$ by evaluating the average values or moments,

$$\langle E^k \rangle = \sum_{i\in\mathscr{C}} g_i E_i^k \Big/ \sum_{i\in\mathscr{C}} g_i, \tag{1}$$

where $g_i$ is the degeneracy of level $i$. The importance of the calculation of such quantities in spectroscopic analysis has been stressed decades ago by Moszkowski [3]. Application of averaging techniques to the computation of opacity of a high-temperature and high-density gold plasma has been proposed by Nardi and Zinamon [4]. The knowledge of energy moments is essential when considering plasmas at local thermodynamical equilibrium, being involved, for instance, in quantities like partition functions, or in the Saha-Boltzmann equation. Beyond the average energy of a configuration [5] given by the $k = 1$ moment in Eq. (1), expressions have been published for the variance ($k = 2$) [6,7]. Concerning higher-order moments, formal methods have been proposed [8], and explicit expressions given for the third-order moment [9]. However, for $k \geqslant 4$ the available literature is rather scarce. In this work our purpose is to consider the moments of the energy distribution defined by Eq. (1) and related to the *spin-orbit* interaction for higher $k$ values, considering mostly highly charged ions for which this interaction rules the electron-electron interaction. Similar to what was reported for transition arrays, we will show here that the energy spectrum cannot be correctly reproduced by lowest-order moments, which motivates the present study about higher orders. More precisely the computation of these distribution moments is useful when analyzing the convergence of the Gram-Charlier expansion. In this work we intend to establish that such expansion can conveniently describe spin-orbit energy spectrum provided that high-order moments as well as some broadening process are included in this spectrum.

This paper is organized as follows. Section II is devoted to the computation of the moments of spin-orbit energy in uncoupled (Sec. II A) and coupled (Sec. II B) scheme, respectively. Comparisons between energy moments obtained from the present analytical expressions and from Cowan's code are then proposed in Sec. III. The convergence of the Gram-Charlier expansion is studied in Sec. IV. Concluding remarks are finally given. Computational details about spin-orbit moments in a monoelectronic configuration and high-order moments are provided in the Appendices, as well as a discussion about moments associated to electron interaction.

## II. ANALYTICAL DETERMINATION OF SPIN-ORBIT MOMENTS

### A. Moments in uncoupled scheme

#### *1. Averaging method*

The calculation of the average of the $k$th power of the atomic Hamiltonian on a $N$-electron configuration relies on the use of the Uylings theorem [10] (see also Appendix in Ref. [6]).

*michel.poirier@cea.fr

 

Using second-quantization techniques [11] it is shown that the average of a $k$-particle operator $O_k$ on a $N$-electron configuration may be derived from the average computed on the $k$-electron configuration using the relation

$$\langle O_k\rangle_N = \binom{N}{k}\langle O_k\rangle_k, \tag{2}$$

where $\binom{N}{k}$ is the binomial coefficient. In this work we will mostly consider single subshell configurations $nl^N$. The case of multiple open subshells will be briefly addressed in Sec. III B. The average values in Eq. (2) are obtained by summing the expression $\langle\phi_k|O_k|\phi_k\rangle$ over all antisymmetric states $\phi_k$ in the configuration $nl^k$ and then dividing it by the number of states $g_k = \binom{4l+2}{k}$. The numerator is the *trace* of the operator and therefore may be computed in any basis. If the quantum numbers of the $j$th electron are noted $q_j$, the $g_k$ elements involved in the trace are defined by the set $(q_1,q_2,\dots q_k)$ where all $q_j$ are different and ordered. Accounting for antisymmetrization of the wave function, the trace is

$$\mathrm{Tr}\, O_k = \binom{4l+2}{k}\langle O_k\rangle_k = \sum_{q_1<\cdots<q_k} f(q_1\dots q_k), \tag{3a}$$

$$f(q_1\dots q_k) = \sum_{\tau\in\mathcal{S}_k}\varepsilon_\tau\langle q_1\dots q_k|O_k|q_{\tau(1)}\dots q_{\tau(k)}\rangle, \tag{3b}$$

where $\mathcal{S}_k$ is the group of permutations of $k$ elements and $\varepsilon_\tau$ is the signature of the permutation $\tau$. In Eq. (3a) the sum index $q_1<\cdots<q_k$ means that each set is counted only once. The computation of such a trace is significantly simplified by noting that the summed quantity $f$ is fully symmetric in the exchange of any pair of indexes $f(q_1,q_2\dots) = f(q_2,q_1\dots)$ and that because of the sum $\sum_{\tau\in\mathcal{S}_k}\varepsilon_\tau$, $f$ vanishes if two indexes are equal $f(q_1,q_1\dots) = 0$. This implies that

$$\mathrm{Tr}\, O_k = \frac{1}{k!}\sum_{q_1\dots q_k} f(q_1\dots q_k). \tag{4}$$

So the sum over nonrepeated indexes may be replaced by the sum where $q_1\dots q_k$ vary freely, which is much more convenient to perform.

The total Hamiltonian in semirelativistic approximation is written as

$$H = \sum_i\left(\frac{p_i^2}{2} - \frac{Z}{r_i}\right) + V_{\mathrm{ee}} + V_{\mathrm{so}}, \tag{5a}$$

with the electron-electron interaction

$$V_{\mathrm{ee}} = \sum_{i<j}\frac{1}{r_{ij}} \tag{5b}$$

and the spin-orbit interaction

$$V_{\mathrm{so}} = \sum_i \xi(r_i)\boldsymbol{l_i}\cdot\boldsymbol{s_i}. \tag{5c}$$

In this paper we intend to obtain the moments $\langle V_{\mathrm{so}}^k\rangle$ for a series of $k$ values. The moment $k=1$ is clearly null, and the variance $\Delta V_{\mathrm{so}}^2$ is well known (see, e.g., Ref. [7]):

$$\kappa_2(\mathrm{so}) = \left\langle V_{\mathrm{so}}^2\right\rangle = \frac{l(l+1)}{4(4l+1)}N(4l+2-N)\langle\xi\rangle^2. \tag{6}$$

Simple expressions can be provided for the next moments, namely the skewness ($k=3$) and kurtosis ($k=4$) for which some computational details follow. Results for $k=5,6$ obtained with the trace method will be given too.

#### 2. *Application to the computation of skewness*

The cube of the spin-orbit interaction Eq. (5c) involves three terms:

$$V_{\mathrm{so}}^3 = S_1 + S_2 + S_3, \tag{7a}$$

$$S_1 = \sum_i(\xi_i\boldsymbol{l_i}\cdot\boldsymbol{s_i})^3, \tag{7b}$$

$$S_2 = 3\sum_{i<j}[(\xi_i\boldsymbol{l_i}\cdot\boldsymbol{s_i})^2\xi_j(\boldsymbol{l_j}\cdot\boldsymbol{s_j}) + i\leftrightarrow j], \tag{7c}$$

$$S_3 = 6\sum_{i<j<k}(\xi_i\boldsymbol{l_i}\cdot\boldsymbol{s_i}\ \xi_j\boldsymbol{l_j}\cdot\boldsymbol{s_j}\ \xi_k\boldsymbol{l_k}\cdot\boldsymbol{s_k}). \tag{7d}$$

The radial part for the considered subshell $\langle\xi_i\rangle^3 = \langle nl|\xi(r)|nl\rangle^3$ is a common factor in all these formulas and will be dropped unless mentioned. One may obtain the average values or traces of each of these operators using Uylings theorem Eq. (2). For instance, the $S_1$ average value will be calculated for $N=1$. One first computes the trace and then divides it by $2(2l+1)$ to get $\langle S_1\rangle_1$. If $N=1$ the uncoupled basis states are $nl\mu_1\sigma_1$, where the magnetic quantum numbers satisfy $-l\leqslant\mu_1\leqslant l$, $-1/2\leqslant\sigma_1\leqslant+1/2$. From the average value Eq. (A3c), one gets immediately

$$\mathrm{Tr}(S_1) = \sum_{\mu_1\sigma_1}\langle\mu_1\sigma_1|(\boldsymbol{l_1}\cdot\boldsymbol{s_1})^3|\mu_1\sigma_1\rangle = -2(2l+1)\frac{l(l+1)}{8}. \tag{8}$$

The trace of two-particle operator Eq. (7c) is calculated similarly. For symmetry reasons both terms inside the brackets give the same contribution. The $1/k!$ factor in Eq. (4) compensates this factor 2, so that, writing explicitly the permutations $\tau$ and dropping unneeded single-electron indexes,

$$\mathrm{Tr}(S_2) = 3(d_2 - e_2), \tag{9a}$$

$$d_2 = \sum_{\substack{\mu_1\sigma_1\\ \mu_2\sigma_2}}\langle\mu_1\sigma_1|(\boldsymbol{l}\cdot\boldsymbol{s})^2|\mu_1\sigma_1\rangle\langle\mu_2\sigma_2|\boldsymbol{l}\cdot\boldsymbol{s}|\mu_2\sigma_2\rangle, \tag{9b}$$

$$e_2 = \sum_{\substack{\mu_1\sigma_1\\ \mu_2\sigma_2}}\langle\mu_1\sigma_1|(\boldsymbol{l}\cdot\boldsymbol{s})^2|\mu_2\sigma_2\rangle\langle\mu_2\sigma_2|\boldsymbol{l}\cdot\boldsymbol{s}|\mu_1\sigma_1\rangle. \tag{9c}$$

The direct term $d_2$ is, up to a constant, the product of average values $\langle(\boldsymbol{l}\cdot\boldsymbol{s})^2\rangle\langle\boldsymbol{l}\cdot\boldsymbol{s}\rangle$, the second of which vanishes. The exchange term $e_2$ is easily derived from the closure relation

$$\sum_{\mu\sigma}|\mu\sigma\rangle\langle\mu\sigma| = 1, \tag{9d}$$

and using again the average value Eq. (A3c), one gets the trace

$$\mathrm{Tr}(S_2) = -3e_2 = -3\sum_{\mu_1\sigma_1}\langle\mu_1\sigma_1|(\boldsymbol{l}\cdot\boldsymbol{s})^3|\mu_1\sigma_1\rangle$$
$$= \frac{3}{4}(2l+1)l(l+1). \tag{9e}$$

In the computation of the trace of the operator Eq. (7d), one has to perform the sum over the 3! permutations of $\mathcal{S}_3$. If any permutation lets one index invariant, e.g., $\tau(3) = 3$, its contribution to the trace cancels since it involves the sum $\langle\mu_3\sigma_3|\boldsymbol{l}\cdot\boldsymbol{s}|\mu_3\sigma_3\rangle$. Therefore, only the two third-order cycles contribute to $\mathrm{Tr}(S_3)$, and for symmetry reasons their contributions are equal. Using Eqs. (7d) and (4), and closure relations, one readily gets

$$\mathrm{Tr}(S_3) = 2\sum_{\substack{\mu_1\mu_2\mu_3\\ \sigma_1\sigma_2\sigma_3}}\langle\mu_1\sigma_1|\boldsymbol{l}\cdot\boldsymbol{s}|\mu_2\sigma_2\rangle\langle\mu_2\sigma_2|\boldsymbol{l}\cdot\boldsymbol{s}|\mu_3\sigma_3\rangle$$
$$\times\langle\mu_3\sigma_3|\boldsymbol{l}\cdot\boldsymbol{s}|\mu_1\sigma_1\rangle \tag{10a}$$
$$= 2\sum_{\mu_1\sigma_1}\langle\mu_1\sigma_1|(\boldsymbol{l}\cdot\boldsymbol{s})^3|\mu_1\sigma_1\rangle \tag{10b}$$
$$= 4(2l+1)\langle(\boldsymbol{l}\cdot\boldsymbol{s})^3\rangle = -\frac{1}{2}l(l+1)(2l+1), \tag{10c}$$

which show that all elements of $\langle V_{\mathrm{so}}^3\rangle$ are reducible to the single-electron average Eq. (A3c). According to Uylings theorem,

$$\langle V_{\mathrm{so}}^3\rangle = \sum_{j=1}^{3}\binom{N}{j}\mathrm{Tr}(S_j)\Big/\binom{4l+2}{j}, \tag{11}$$

and from Eqs. (8), (9e), and (10c) one gets the contribution of spin-orbit interaction to the configuration skewness,

$$\langle V_{\mathrm{so}}^3\rangle_N = \langle\xi\rangle^3\frac{(l+1)}{16(4l+1)}N(4l+2-N)(N-2l-1). \tag{12}$$

This expression agrees with the result from Kučas and Karazija [9]. As expected the skewness vanishes for an empty or closed subshell. It depends on $M = N-2l-1$ as $M[M^2-(2l+1)^2]$. More generally one may easily check that $V_{\mathrm{so}}^{2k+1}$ (respectively, $V_{\mathrm{so}}^{2k}$) is an odd (respectively, even) function of $M$. A proof is given in Sec. II B.

### 3. *Application to kurtosis*

Expanding the fourth power of the spin-orbit interaction, one gets

$$V_{\mathrm{so}}^4 = K_1 + K_2 + K_2' + K_3 + K_4, \tag{13a}$$
$$K_1 = \sum_i(\xi_i\boldsymbol{l_i}\cdot\boldsymbol{s_i})^4, \tag{13b}$$
$$K_2 = 4\sum_{i<j}[(\xi_i\boldsymbol{l_i}\cdot\boldsymbol{s_i})^3\xi_j(\boldsymbol{l_j}\cdot\boldsymbol{s_j}) + i\leftrightarrow j], \tag{13c}$$
$$K_2' = 6\sum_{i<j}(\xi_i\boldsymbol{l_i}\cdot\boldsymbol{s_i})^2(\xi_j\boldsymbol{l_j}\cdot\boldsymbol{s_j})^2, \tag{13d}$$
$$K_3 = 12\sum_{i<j<k}[(\xi_i\boldsymbol{l_i}\cdot\boldsymbol{s_i})^2\,\xi_j\boldsymbol{l_j}\cdot\boldsymbol{s_j}\,\xi_k\boldsymbol{l_k}\cdot\boldsymbol{s_k} + (ijk) + (ikj)], \tag{13e}$$
$$K_4 = 24\sum_{i<j<k<m}\xi_i\boldsymbol{l_i}\cdot\boldsymbol{s_i}\,\xi_j\boldsymbol{l_j}\cdot\boldsymbol{s_j}\,\xi_k\boldsymbol{l_k}\cdot\boldsymbol{s_k}\xi_m\,\boldsymbol{l_m}\cdot\boldsymbol{s_m}, \tag{13f}$$

where in Eq. (13e) $(ijk)$,$(ikj)$ stands for the cyclic permutations of indexes.

Using the same techniques as above, one gets, after computing the sum over the permutations in $\mathcal{S}_k$,

$$\mathrm{Tr}(K_1)\Big/\binom{4l+2}{1} = \langle K_1\rangle_1 = m_4, \tag{14a}$$
$$\mathrm{Tr}(K_2)\Big/\binom{4l+2}{2} = \langle K_2\rangle_2 = -\frac{8m_4}{4l+1}, \tag{14b}$$
$$\mathrm{Tr}(K_2')\Big/\binom{4l+2}{2} = \langle K_2'\rangle_2 = \frac{6}{4l+1}\big[2(2l+1)m_2^2 - m_4\big], \tag{14c}$$
$$\mathrm{Tr}(K_3)\Big/\binom{4l+2}{3} = \langle K_3\rangle_3 = \frac{18}{l(4l+1)}\big[-(2l+1)m_2^2 + m_4\big], \tag{14d}$$
$$\mathrm{Tr}(K_4)\Big/\binom{4l+2}{4} = \langle K_4\rangle_4 = \frac{36}{l(4l-1)(4l+1)}\big[(2l+1)m_2^2 - m_4\big], \tag{14e}$$

where the one-electron average values,

$$m_n = \langle(\boldsymbol{l}\cdot\boldsymbol{s})^n\rangle, \tag{15}$$

are detailed in Appendix A. The average values of these operators for a $N$-electron configuration are obtained using Uylings theorem Eq. (2) and one gets after some algebra the expression of the fourth moment,

$$\langle V_{\mathrm{so}}^4\rangle_N = \langle\xi\rangle^4\frac{(l+1)N(4l+2-N)}{32(4l-1)(4l+1)}f_4, \tag{16a}$$
$$\text{with } f_4 = 2l(2l+1)^2(3l^2+l-1) - 3(2l^3+2l^2-1)(N-2l-1)^2 \tag{16b}$$
$$= 2l(4l-1)(l^2+l+1) + 3(2l^3+2l^2-1)(N-1)(4l+1-N). \tag{16c}$$

The fourth-order cumulant, sometimes called "excess," which measures the sharpness of the distribution, is defined as

$$\kappa_4(\mathrm{so}) = \langle V_{\mathrm{so}}^4\rangle - 3\langle V_{\mathrm{so}}^2\rangle^2. \tag{17}$$

A negative (respectively, positive) value indicates a distribution flatter (respectively, sharper) than a Gaussian profile.

Using the known value of the variance Eq. (6), one gets

$$\kappa_4(\mathrm{so}) = -\frac{(l+1)N(4l+2-N)}{32(4l-1)(4l+1)^2}k_4, \tag{18a}$$

with

$$k_4 = 2l(2l+1)^2(2l^2+1) + c_4(N-2l-1)^2, \tag{18b}$$

$$c_4 = 3(4l^3+4l^2-4l-1), \tag{18c}$$

and since $4l^3+4l^2-4l-1>0$ for $l>0$, as seen from Eq. (18b) the factor $k_4$ is also positive. This proves that the excess is negative, which means that the spin-orbit distribution is flatter than a Gaussian profile.

#### *4. Application to higher-order moments*

Using the same techniques, we have computed the next average values. The result for $k=5$ is

$$\left\langle V_{\mathrm{so}}^5\right\rangle_N = -\langle\xi\rangle^5\frac{(l+1)(2l+1-N)N(4l+2-N)}{64(4l-1)(4l+1)}f_5, \tag{19a}$$

$$\text{with } f_5 = (2l+1)^2(10l^2+6l-1) - 2(5l^2+7l+3)(N-2l-1)^2. \tag{19b}$$

Finally, for $k=6$ one gets

$$\left\langle V_{\mathrm{so}}^6\right\rangle_N = \langle\xi\rangle^6\frac{(l+1)N(4l+2-N)}{128(4l-3)(4l-1)(4l+1)}f_6, \tag{20a}$$

$$\begin{aligned}\text{with } f_6 = {} & 2l(2l+1)^4(15l^4-14l^2-l+3)\\ & -5(2l+1)^2(12l^5+12l^4-6l^3\\ & -19l^2-5l+3)(N-2l-1)^2\\ & +5(6l^5+12l^4+6l^3-13l^2\\ & -17l-6)(N-2l-1)^4.\end{aligned} \tag{20b}$$

However, this method becomes cumbersome when dealing with high-order moments because it is necessary to account for $k$-particle interaction and for the whole set of permutations $\mathcal{S}_k$. That is why we have implemented an alternative method of derivation using coupled moments.

### B. Computation of moments in coupled scheme

#### *1. General formulas*

Using the eigenvectors of the operators $j_i^2$ and $j_{iz}$ noted as $\{j_i m_i\}(i=1\ldots N)$, a $N$-electron state obeying Pauli principle is defined by the occupation number $\nu$ for the total angular momentum $j=l-1/2$, by the set of $\nu$ distinct values $m_1^-,\ldots m_\nu^-$, and by the set of $N-\nu$ distinct values $m_1^+,\ldots m_{N-\nu}^+$ for $j=l+1/2$. The number of allowed states is given by the possible choice of $\nu$ magnetic quantum numbers among $2l$ and $N-\nu$ magnetic quantum numbers among $2l+2$, i.e.,

$$g(N,\nu,l) = \binom{2l}{\nu}\binom{2l+2}{N-\nu}. \tag{21}$$

Since the spin-orbit Hamiltonian is diagonal in this basis, the energy of a relativistic configuration of populations $\nu$, $N-\nu$ is straightforwardly obtained as

$$E_{\mathrm{so}} = \frac{\langle\xi\rangle}{2}[Nl-(2l+1)\nu]. \tag{22}$$

The radial term $\langle\xi\rangle$ identical for all states in a configuration will be omitted in the following formulas. The average $k$th power of spin-orbit energy is, therefore,

$$\left\langle V_{\mathrm{so}}^k\right\rangle_N = \frac{1}{2^k\binom{4l+2}{N}}\sum_\nu\binom{2l}{\nu}\binom{2l+2}{N-\nu}[Nl-(2l+1)\nu]^k. \tag{23}$$

Such average values are computed using the identity

$$\sum_\nu\binom{M}{\nu}\binom{N}{k-\nu}\frac{\nu!}{(\nu-p)!} = \frac{M!}{(M-p)!}\binom{M+N-p}{k-p}, \tag{24}$$

derived from the Taylor expansion of $M(M-1)\ldots(M-p+1)(1+X)^{M+N-p}$. In order to use this formula one has to express the term $[Nl-(2l+1)X]^k$ in Eq. (23) as a function of the polynomials

$$\phi_j(\nu) = \nu(\nu-1)\ldots(\nu-j+1), \text{ with } \phi_0(\nu)=1. \tag{25}$$

Writing any $k$th degree polynomial as

$$P_k(X) = \sum_{j=0}^k c_j^{(k)}\phi_j(X) \tag{26}$$

for $X=0,1\ldots k$ successively, one gets a set of $k+1$ linear equations, which can be readily solved for the $c_j^{(k)}$,

$$c_j^{(k)} = \frac{1}{j!}\sum_{i=0}^j(-1)^{j-i}\binom{j}{i}P_k(i). \tag{27}$$

Identifying $P_k(X)$ with $[Nl-(2l+1)X]^k$, one can then write the moment Eq. (23) using its definition and Eq. (27),

$$\begin{aligned}\left\langle V_{\mathrm{so}}^k\right\rangle_N = {} & \frac{2^{-k}}{\binom{4l+2}{N}}\sum_{j=0}^{j_{\max}}\frac{(2l)!}{(2l-j)!}\binom{4l+2-j}{N-j}\\ & \times\sum_{i=0}^j\frac{(-1)^{j-i}}{i!(j-i)!}[Nl-(2l+1)i]^k\end{aligned} \tag{28a}$$

$$\begin{aligned} = {} & 2^{-k}\sum_{j=0}^{j_{\max}}\frac{(2l)!(4l+2-j)!N!}{(2l-j)!(4l+2)!(N-j)!}\\ & \times\sum_{i=0}^j\frac{(-1)^{j-i}}{i!(j-i)!}[Nl-(2l+1)i]^k,\end{aligned} \tag{28b}$$

with

$$j_{\max} = \min(k,2l,N). \tag{28c}$$

This expression is apparently more complex than Eq. (23) since it involves a double sum. In fact, since $0\leqslant i\leqslant j\leqslant k$, for the lowest $k$ values very few terms have to be computed, and this number of terms—at maximum $k+1$ values for $j$ and $(k+1)(k+2)/2$ values for $i$—is independent of the number of electrons $N$ in the subshell. Besides, this formula is easy to implement in a formal algebra software such as Mathematica. On Eq. (23), one readily verifies that changing $\nu$ in $2l-\nu$ and

$N-\nu$ in $2l+2-(N-\nu)$ and therefore $N$ in $4l+2-N$, the contribution of this subshell to the moment is multiplied by $(-1)^k$. This shows that

$$\langle V_{\rm so}^k\rangle_{4l+2-N} = (-1)^k \langle V_{\rm so}^k\rangle_N, \tag{29}$$

a property that was obviously verified on the various $\langle V_{\rm so}^k\rangle$ moments detailed in the previous subsection. Examples of application of Eq. (28b) are given in the following subsection.

#### 2. *Explicit expression for high-order moments using coupled basis*

Using the double sum formula Eq. (28b) for the moment $\langle V_{\rm so}^k\rangle$, and defining $M = N - 2l - 1$, one easily obtains analytical expressions for $k > 6$, namely

$$\langle V_{\rm so}^7\rangle = \frac{(l+1)N(4l+2-N)(N-2l-1)}{512(4l-3)(4l-1)(4l+1)}[A_7(l)+B_7(l)M^2+C_7(l)M^4], \tag{30a}$$

$$\text{with } A_7(l) = 2(2l+1)^4(105l^4+56l^3-55l^2-28l+3), \tag{30b}$$

$$B_7(l) = -5(2l+1)^2(84l^4+140l^3+64l^2-21l-18), \tag{30c}$$

$$C_7(l) = 3(70l^4+196l^3+234l^2+133l+30), \tag{30d}$$

$$\langle V_{\rm so}^8\rangle = \frac{(l+1)N(4l+2-N)}{1024(4l-5)(4l-3)(4l-1)(4l+1)}[A_8(l)+B_8(l)M^2+C_8(l)M^4+D_8(l)M^6], \tag{31a}$$

$$A_8(l) = 4l(2l+1)^6(105l^6-105l^5-147l^4+85l^3+87l^2-13l-15), \tag{31b}$$

$$B_8(l) = -14(2l+1)^4(90l^7+30l^6-162l^5-248l^4+38l^3+182l^2+40l-15), \tag{31c}$$

$$C_8(l) = 35(2l+1)^2(36l^7+60l^6-12l^5-196l^4-208l^3-20l^2+73l+30), \tag{31d}$$

$$D_8(l) = -7(60l^7+180l^6+180l^5-280l^4-888l^3-932l^2-459l-90), \tag{31e}$$

$$\langle V_{\rm so}^9\rangle = \frac{(l+1)N(4l+2-N)(N-2l-1)}{1024(4l-5)(4l-3)(4l-1)(4l+1)}[A_9(l)+B_9(l)M^2+C_9(l)M^4+D_9(l)M^6], \tag{32a}$$

$$\text{with } A_9(l) = (2l+1)^6(1260l^6-252l^5-1770l^4-332l^3+564l^2+182l-15), \tag{32b}$$

$$B_9(l) = -7(2l+1)^4(540l^6+684l^5-204l^4-886l^3-468l^2+43l+60), \tag{32c}$$

$$C_9(l) = 7(2l+1)^2(540l^6+1476l^5+1530l^4+244l^3-786l^2-625l-150), \tag{32d}$$

$$D_9(l) = -2(630l^6+2646l^5+5184l^4+5773l^3+3777l^2+1361l+210), \tag{32e}$$

$$\langle V_{\rm so}^{10}\rangle = \frac{(l+1)N(4l+2-N)}{4096(4l-7)(4l-5)(4l-3)(4l-1)(4l+1)}[A_{10}(l)+B_{10}(l)M^2 + C_{10}(l)M^4+D_{10}(l)M^6+E_{10}(l)M^8], \tag{33a}$$

$$\text{with } A_{10}(l) = 4l(2l+1)^8(945l^8-2520l^7+3090l^5+226l^4-1594l^3-484l^2+241l+105), \tag{33b}$$

$$B_{10}(l) = -6(2l+1)^6(2520l^9-2520l^8-7140l^7-4450l^6+13410l^5 + 13126l^4-4286l^3-6819l^2-1051l+315), \tag{33c}$$

$$C_{10}(l) = 21(2l+1)^4(1080l^9+720l^8-3000l^7-9300l^6-3560l^5 + 10564l^4+12051l^3+2459l^2-2074l-840), \tag{33d}$$

$$D_{10}(l) = -42(2l+1)^2(360l^9+840l^8+60l^7-4410l^6-8450l^5-4918l^4 + 3083l^3+6007l^2+3243l+630), \tag{33e}$$

$$E_{10}(l) = 9(420l^9+1680l^8+2520l^7-3220l^6-18760l^5-33476l^4 - 32829l^3-18951l^2-6074l-840). \tag{33f}$$

TABLE I. Absolute and scaled centered moments of energy distribution for the $3d^6$ configuration in $Au^{55+}$ with an Ar-like core. The results from Cowan's code are computed both with the complete interaction ($V_{ee}, V_{so}$) and with only spin-orbit terms ($V_{so}$). The notation 1.195(8) stands for $1.195 \times 10^8$. Analytical values of moments including the whole interaction are not available at any order; however, values for $n = 2$ and 3 are given in the main text.

| | Cowan's code | | | This work | |
|---|---|---|---|---|---|
| | Centered moment | | Scaled moment | Centered moment | Scaled moment |
| $n$ | $\mu_n(V_{ee}, V_{so})$ | $\mu_n(V_{so})$ | $\alpha_n(V_{so})$ | $\mu_n(V_{so})$ | $\alpha_n(V_{so})$ |
| 2 | 6692 | 6357 | 1 | 6356.87 | 1 |
| 3 | 8111 | 3.168(4) | 0.062500 | 3.16771(4) | 0.0625 |
| 4 | 1.195(8) | 1.11(8) | 2.747768 | 1.11037(8) | 2.7477679 |
| 5 | 7.187(8) | 2.16(9) | 0.670201 | 2.15930(9) | 0.67020089 |
| 6 | 3.128(12) | 2.929(12) | 11.399971 | 2.92843(12) | 11.399972 |
| 7 | 7.351(13) | 1.427(14) | 6.968505 | 1.42722(14) | 6.9685059 |
| 8 | 1.002(17) | 9.738(16) | 59.621394 | 9.73590(16) | 59.621399 |
| 9 | 6.277(18) | 9.73(18) | 74.722146 | 9.72849(18) | 74.722153 |
| 10 | 3.824(21) | 3.999(21) | 385.137765 | 3.99792(21) | 385.13780 |

## III. MOMENT ANALYSIS: COMPARISON BETWEEN ANALYTICAL EXPRESSIONS AND NUMERICAL COMPUTATIONS

In this section we compare computations of centered moments $\mu_n = \langle (E - \langle E \rangle)^n \rangle$ from Cowan's code [5] to the proposed analytical expressions. An option in Cowan's code allows one to cancel the electron-electron interaction, leading to an energy structure depending on spin-orbit interaction only. We first compare the spin-orbit energy moments computed with the present analytical formulas to the numerical results from Cowan's code, considering the case of the $3d^6$ configuration. The case of two open subshells is considered next.

### A. Analysis of moments for a single open subshell

As a first example we present in Table I the moments up to $n = 10$ for the $3d^6$ configuration in $Au^{55+}$ with an Ar-like core. The Cowan's code provides the spin-orbit integral $\langle \xi \rangle_{3d} = 39.865$ eV. The variance derived from the analytical form, Eq. (6), is 6356.9 $eV^2$, which fairly agrees with the numerical determination from Cowan's code of 6357 $eV^2$ as listed in Table I. The various higher-order moments are listed in this table, first as absolute values $\mu_n$, and as scaled values $\alpha_n$, i.e., divided by $\sigma^n$, where $\sigma^2$ is the variance. The last two columns are obtained with the analytical expressions given above.

In Table I it appears that the spin-orbit moments computed with Cowan's code fairly agree with the present determination at any order, as absolute as well as scaled values. We note on columns 2 and 3 that including the electronic interaction mostly affects the low- and even-order moments. We do not have a definite explanation for this feature, but we may empirically state that electron-electron interaction contributes more significantly than spin-orbit to the asymmetry of energy structure.

Furthermore, one may evaluate analytically the moments for $n$ up to 3 in the case where electronic interaction is also accounted for. The Cowan's code provides for the Slater integrals the following values: $F^{(2)}(3d,3d) = 75.677$ eV and $F^{(4)}(3d,3d) = 48.937$ eV. Inserting these values in the formulas for the variance available in the literature (Table 3.2 in Ref. [7]) we get $\langle (V_{ee} - \langle V_{ee} \rangle)^2 \rangle = 334.7$ $eV^2$ and $\langle V_{so}^2 \rangle = 6356.9$ $eV^2$, the total variance being 6691.6 $eV^2$. This variance fairly agrees with the one in Table I. The analysis of third-order moment including electron-electron interaction is presented in Appendix B. The derivation of moments including both $V_{ee}$ and $V_{so}$ is outside the scope of this paper and would be a tremendous task with probably page-long formulas if $n > 3$.

### B. Ion with two open subshells

More complex configurations with several open subshells $n_1 l_1^{p_1} n_2 l_2^{p_2} \ldots$ can be dealt with using cumulants (see, e.g., Refs. [12,13]). In the case where *centered* moments $\mu_j = \langle (E - E_{av})^j \rangle$ are used, the first cumulants get simple expressions,

$$\kappa_2 = \mu_2, \quad \kappa_3 = \mu_3, \quad \kappa_4 = \mu_4 - 3{\mu_2}^2, \\ \kappa_5 = \mu_5 - 10\mu_3\mu_2, \tag{34}$$

and are more generally given by the recursion relation,

$$\kappa_n = \mu_n - \sum_{m=1}^{n-1} \binom{n-1}{m-1} \mu_{n-m}\kappa_m. \tag{35}$$

The cumulant $\kappa_2$ is simply the variance $\sigma^2$ of the distribution. The interest of these quantities versus the ordinary moments is that the cumulants are additive if two phenomena are statistically independent. In the case of multiple opened subshells, the cumulants computed for each subshell add up for the spin-orbit part, provided that the spin-orbit interaction does not couple different subshells. This result does not apply to the electronic interaction $V_{ee}$. For instance, the variance accounting for this interaction is a function of Slater integrals involving distinct subshells [7].

In order to illustrate the case of two open subshells we present in Table II the moments up to $n = 6$ for the $3p^2 3d^6$ configuration in $Au^{59+}$ with a Mg-like core. In addition to the centered moments, the cumulants defined in Eq. (34) have

TABLE II. Centered moments and cumulants for the levels of $3p^2 3d^6$ configuration in $Au^{59+}$ with a Mg-like core. Columns 2 and 3 contain the centered moments $\mu_n$ obtained with Cowan's code, with electron interaction, respectively, included or not. Column 4 gives the list of cumulants $\kappa_n$, Eq. (34), derived from Cowan's data with only spin-orbit included. The three rightmost columns are computations using the spin-orbit parameter provided by the Cowan's code and the present analytical formulas. The tabulated cumulants refer to the $3p^2$ subshell, the $3d^6$ subshell, and the whole configuration for columns 5–7, respectively. All data relative to order $n$ are in units of $eV^n$. The notation 9.26(4) stands for $9.26 \times 10^4$.

| | Data from Cowan's code | | | Cumulants from analytical formulas | | |
|---|---|---|---|---|---|---|
| $n$ | $\mu_n(V_{ee}, V_{so})$ | $\mu_n(V_{so})$ | $\kappa_n(V_{so})$ | $\kappa_n(3p^2)$ | $\kappa_n(3d^6)$ | $\kappa_n$ total |
| 2 | 9.48(4) | 9.26(4) | 9.26(4) | 8.546(4) | 7.144(3) | 9.260(4) |
| 3 | − 7.332(6) | − 6.945(6) | − 6.945(6) | − 6.983(6) | 3.774(4) | − 6.945(6) |
| 4 | 2.171(10) | 2.092(10) | − 4.804(9) | − 4.793(9) | − 1.287(7) | − 4.806(9) |
| 5 | − 7.394(12) | − 6.991(12) | − 5.599(11) | − 5.595(11) | 1.950(8) | − 5.593(11) |
| 6 | 8.23(15) | 7.712(15) | 1.992(15) | 1.993(15) | 5.265(10) | 1.993(15) |

been extracted from Cowan's data. The spin-orbit parameters $\langle\xi\rangle$ are 326.842 eV and 42.261 eV for $3p$ and $3d$ subshells, respectively. With the present analytical formulas for $\langle V_{so}^n\rangle$ we have computed the cumulants Eq. (34) for each subshell separately and their sums. In Table II we verify that the sum of the contributions of each subshell is in fair agreement with the cumulant derived from Cowan's data. However, when the order $n$ increases, since each cumulant is proportional to $\langle\xi\rangle^n$, the $3p$ subshell has a much larger contribution than the $3d$ subshell, and the additivity property loses its significance. That is why we restrict the analysis to $n \leqslant 6$.

Contrary to what we observed in the previous subsection, the moments involving $V_{ee}$ and $V_{so}$ (column 2 of Table II) do not differ much from the moments involving $V_{so}$ only (column 3), whatever the order. This is because we consider here a configuration $3p^2 3d^6$ while the previous case involved only $d$ electrons. As a rule, the spin-orbit integral decreases more rapidly with the angular momentum $l$ than the Slater integrals.

## IV. ANALYSIS OF GRAM-CHARLIER EXPANSION

### A. Standard analysis

In this section we try to model the energy distribution by a Gram-Charlier type A distribution [12], quite popular among statisticians, and which involves in a simple way moments of any order. This distribution, truncated at index $p$, is

$$F_{GC}(E) = \frac{g}{(2\pi)^{1/2}\sigma}\exp\left[-\frac{(E-E_{av})^2}{2\sigma^2}\right] \times\left[1+\sum_{n=2}^{p} c_n \mathrm{He}_n\left(\frac{E-E_{av}}{\sigma}\right)\right], \quad (36)$$

where $\mathrm{He}_n$ is the Hermite polynomial [14],

$$\mathrm{He}_n(X) = n!\sum_m \frac{(-1)^m X^{n-2m}}{2^m m!(n-2m)!}, \quad (37)$$

this summation being restricted to $m$ values for which the inverse factorials do not cancel. The distribution Eq. (36) is here normalized to the configuration degeneracy $g$. The Gram-Charlier coefficients $c_n$ are related to the scaled centered moments,

$$\alpha_n = \mu_n/\sigma^n \quad \text{with } \sigma^2 := \mu_2 \text{ (or } \alpha_2 := 1), \quad (38a)$$

by

$$c_n = \sum_j \frac{(-1)^j \alpha_{n-2j}}{2^j j!(n-2j)!}. \quad (38b)$$

The above definitions imply that $c_2 = 0$.

The evolution of the Gram-Charlier expansion Eq. (36) built with the spin-orbit moments for the $3d^6$ configuration of $Au^{55+}$ is shown on Fig. 1 for various truncation indexes $p$. The spectrum built with energies and degeneracies from Cowan's code where $V_{ee}$ is unaccounted for is plotted too, with an arbitrary Lorentzian line shape of 2-eV FWHM. This line shape is included only to facilitate the visual comparison

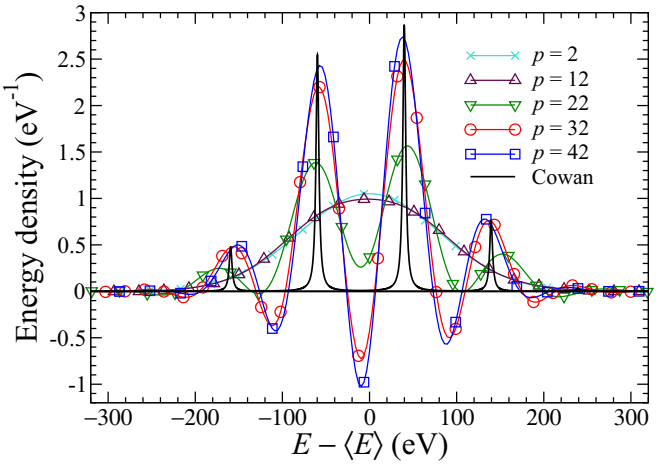


FIG. 1. Gram-Charlier distribution for the spin-orbit energy of the $3d^6$ configuration in $Au^{55+}$ with an Ar-like core. The various curves correspond to the expansions truncated at various indexes $p$. For comparison purpose one has plotted the data from Cowan's code where each energy level is arbitrarily represented by a Lorentzian of 2 eV FWHM not accounted for in the moment computation. The Gram-Charlier curves are normalized to the degeneracy $g = 210$. The ordinates for Cowan's data have been divided by a suitable factor in order to allow comparison.

between distributions but it is not included in the moment computations.

When varying the truncation index $p$ we observed that the case $p = 3$ in the Gram-Charlier expansion is hardly distinguishable from the pure Gaussian case $p = 2$—the difference being below 2%—and for the sake of clarity the $p = 3$ case was not plotted on Fig. 1. The same observation can be made for the next values $p \lesssim 10$. For $p = 12$ some asymmetry appears and increases gradually. The Gram-Charlier expansion is then changing significantly even when $p$ increases by one unit. Two separate components appear in the distribution for $p > 15$. For $p = 22$ the expansion is clearly negative for energies around $-230$ eV and $+230$ eV. The position of the peaks in the Gram-Charlier distribution gets in better agreement with Cowan's data when $p$ increases. Nevertheless, we may check that for indexes $p$ up to 42 no convergence is reached since the expansion still varies significantly.

### B. Convolution procedure

This absence of convergence can be explained and amended as follows. The "theoretical" energy distribution we try to represent by a Gram-Charlier expansion is indeed a "Dirac comb" since no broadening is accounted for on individual components. From a general point of view, the Gram-Charlier expansion is relevant for statistical phenomena such as coalescent transition arrays and not when individual lines show up. In order to verify this point we have performed the convolution of the energy distribution by a Gaussian profile $\exp(-E^2/2\tau^2)/(2\pi)^{(1/2)}\tau$. This can be considered as a mathematical artifact to monitor convergence. More significantly from a physical point of view it may also account for various broadening processes such as Stark broadening or Zeeman effect with a inhomogeneous magnetic field.

In favor of this analysis we mention that the convolution of a Gram-Charlier expansion characterized by variance $\sigma^2$ and coefficients $c_n$ with a Gaussian profile of variance $\tau^2$ is again a Gram-Charlier expansion with variance

$$\upsilon^2 = \sigma^2 + \tau^2 \tag{39a}$$

and coefficients $c'_n = (\sigma/\upsilon)^n c_n$, the convolved function being

$$F'_{\mathrm{GC}}(X) = \frac{g}{(2\pi)^{1/2}\upsilon} e^{-X^2/2\upsilon^2}\left(1 + \sum_n (\sigma/\upsilon)^n c_n \mathrm{He}_n(X/\upsilon)\right). \tag{39b}$$

The scaled moments of the convolved energy distribution $\alpha'_n = \mu'_n/(\mu'_2)^{n/2}$ are related to the transformed coefficients $c'_n$ through an equation formally similar to Eq. (38b). One gets

$$\alpha'_n = \frac{n!\sigma^n}{(\sigma^2+\tau^2)^{n/2}} \sum_j \frac{(\tau/\sigma)^{2j}\alpha_{n-2j}}{2^j\, j!(n-2j)!} \tag{40a}$$

$$= \frac{\pi^{-1/2}}{(\sigma^2+\tau^2)^{n/2}} \sum_k \binom{n}{k} \frac{1+(-1)^{n-k}}{2} \times \sigma^k (2\tau^2)^{(n-k)/2} \Gamma\left(\frac{n-k+1}{2}\right)\alpha_k, \tag{40b}$$

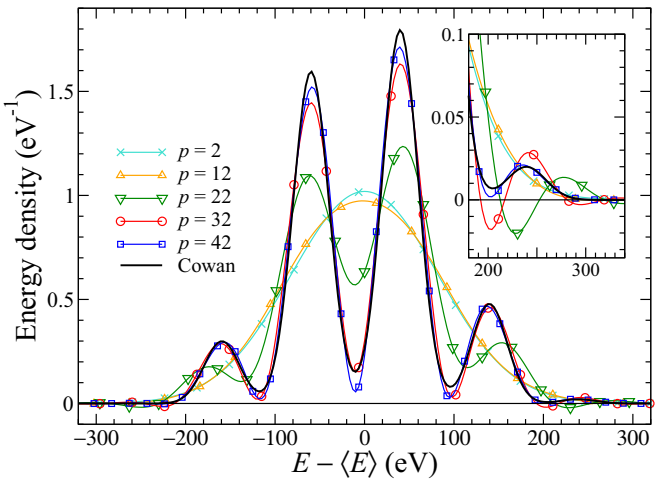


FIG. 2. Gram-Charlier distribution for the spin-orbit energy of the $3d^6$ configuration in $Au^{55+}$ with an Ar-like core convolved by a Gaussian profile with standard deviation $\tau = 20$ eV. The Gram-Charlier curves and Cowan's data are normalized to the degeneracy $g = 210$.

a relation that was previously established by Pain and Gilleron (Eq. (40) in Ref. [15]). The effect of this convolution is illustrated by Fig. 2 with the same Cowan's data as on Fig. 1 and including a convolution by a profile with standard deviation $\tau = 20$ eV, which ensure the coalescence of lines. In this case a good agreement is observed between convolved Cowan's data and Gram-Charlier expansion at order $n \simeq 42$. One also notes that for high enough $n$, the negative part of the energy distribution has almost disappeared. Because of the factor $(\sigma/\upsilon)^n$ in Eq. (39b), increasing the Gaussian width $\tau$ improves the convergence speed.

### C. Convergence analysis

In order to ensure that we did reach convergence in the latter case considered and not in the former, we have plotted on Fig. 3 the absolute value of the coefficients in the Gram-Charlier expansion $t(n) = c_n \mathrm{He}_n(X/\sigma)$ (respectively, $t'(n) = c'_n \mathrm{He}_n(X/\upsilon)$) for the distribution before (respectively, after) convolution. The case considered here is again the $d^6$ configuration with a nonconvolved standard deviation $\sigma = 79.7$ eV and a convolution parameter $\tau = 20$ eV. Computations have been performed at an arbitrary energy $X = 1$ eV, but the results would exhibit the same behavior for any value of $X$. One notes that without convolution, the Gram-Charlier series hardly converges since the term $t(900)$ is about 0.02 in absolute value. The strong oscillations visible on this plot correspond to changes in sign and amplitude of both $c_n$ and $\mathrm{He}_n(X/\sigma)$ factors. Using the asymptotic form of Hermite polynomials [14] one can verify that this second factor is indeed an oscillating function of $n$ with increasing amplitude, while the present numerical analysis shows that $c_n$ is an oscillating function with decreasing amplitude. Using two independent numerical methods—quadruple precision Fortran and Mathematica in arbitrary precision—we could verify that oscillations on Fig. 3 are not a computational artifact. It appears that the Gram-Charlier expansion converges toward

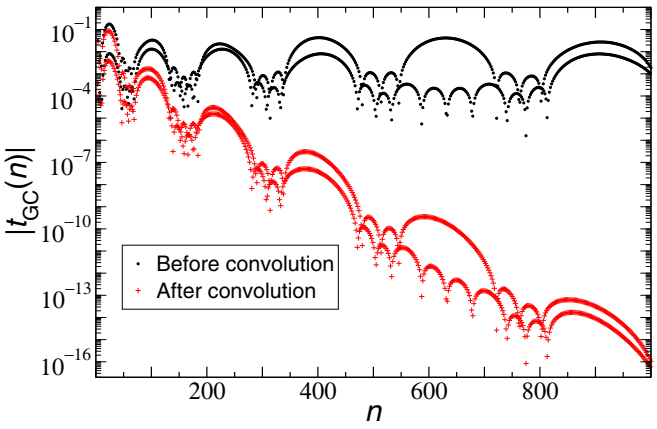


FIG. 3. Absolute value of the Gram-Charlier term series $c_n \mathrm{He}_n(X/\sigma)$ and $c'_n \mathrm{He}_n(X/\upsilon)$ as a function of $n$ for the $d^6$ configuration in $Au^{+55}$. The standard deviation on energy before convolution is $\sigma = 2\xi = 79.7$ eV. The original distribution has been convolved with a Gaussian profile with standard deviation $\tau = 20$ eV. See main text for more details.

the convolved energy distribution, though slowly if the ratio $\sigma/\upsilon$ is close to unity. This slow convergence of the Gram-Charlier distribution is reminiscent of the behavior observed on the $3d^6$-$3d^5 4p$ transition array in bromine by Gilleron and Pain [16]—though no convolution is then required since the array exhibits coalescence. The Gram-Charlier expansion, though slowly or poorly convergent in some cases, is the simplest form available to check the influence of moments at any order. Other distributions have been proposed [17], but they either involve a reduced set of parameters or give rise to tedious formulas for defining their parameters as a function of the moments. This is why we restricted the present analysis to such an expansion.

## V. SUMMARY AND CONCLUSIONS

Using a formalism based on second quantization and angular momentum algebra, we have been able to derive high-order moments for the spin-orbit energy in a $N$-electron system. Contrary to electron-electron interaction, which gives rise to formulas of huge complexity when the order $k$ grows, moments originating from spin-orbit can be expressed analytically through tractable expressions. One must note that, unlike transition-array computations, the configuration averages such as those obtained here are *exact* as far as the semirelativistic description is correct. The invariance of the trace means that computed averages can be compared to numerical or experimental data, an example of such verification being provided by the present work on $3d^6$ configuration. Two methods have been implemented, one based on Uylings theorem and reduction of matrix elements to single-electron elements using closure relations, the other based on coupling of orbital and spin angular momenta and use of analytical expressions. These methods were found to agree in all the tested cases. It was verified that the spin-orbit contribution to the excess (fourth-order cumulant) is always negative, meaning that the energy distribution is flatter than a Gaussian. The current analytical determination for moments up to 10th order agree with computations based on Cowan's code where electron interaction is not accounted for. A corrected formula for the asymmetry originating from electron-electron interaction has been provided and we found that the agreement on the second- and third-order moments is also excellent when the various terms in the Hamiltonian are accounted for. It has been checked that the Gram-Charlier expansion built with moments of spin-orbit energy does not exhibit convergence if no level width is accounted for. However, this series does converge though at high order when a suitable convolution procedure is performed. Finally, using data from Cowan's code we have checked that the electron interaction may in some cases have a more significant effect than spin-orbit on low- and odd-order moments, such as the skewness. This may stimulate further work.

## ACKNOWLEDGMENTS

This work has been partly supported by the European Communities under the contract of Association between EURATOM and CEA within the framework of the European Fusion Program. The authors are grateful to Dr. J.-C. Pain and Dr. F. Gilleron for kindly providing data from Cowan's code and for a series of stimulating discussions. Useful advices from Dr. T. Blenski have also been appreciated.

## APPENDIX A: MOMENTS OF THE SPIN-ORBIT ENERGY IN A SINGLE-ELECTRON CONFIGURATION

We give here values of the average $\langle(\boldsymbol{l}\cdot\boldsymbol{s})^k\rangle$ for a single-electron configuration, dropping the constant radial factor $\xi(r)$,

$$\langle(\boldsymbol{l}\cdot\boldsymbol{s})^k\rangle = \frac{1}{2(2l+1)}\sum_{\mu\sigma}\langle\mu\sigma|(\boldsymbol{l}\cdot\boldsymbol{s})^k|\mu\sigma\rangle. \tag{A1}$$

The most straightforward method lies in using the $ls$ coupled basis $jm$, where the spin-orbit term is diagonal. For $j = l \pm 1/2$ the level degeneracy is $2l$ and $2l+2$, respectively, and the spin-orbit energy $-(l+1)/2$ and $l/2$, respectively, so that

$$\langle(\boldsymbol{l}\cdot\boldsymbol{s})^k\rangle = \frac{1}{2(2l+1)}\sum_{jm}\langle jm\big|(\boldsymbol{l}\cdot\boldsymbol{s})^k\big|jm\rangle, \tag{A2a}$$

$$= \frac{1}{2(2l+1)}\sum_{jm}(j(j+1)-l(l+1)-3/4)^k/2^k, \tag{A2b}$$

$$= \frac{l(l+1)}{2^k(2l+1)}[(-1)^k(l+1)^{k-1}+l^{k-1}]. \tag{A2c}$$

This provides the average values for the first $k$ values

$$\langle\boldsymbol{l}\cdot\boldsymbol{s}\rangle = 0, \tag{A3a}$$

$$\langle(\boldsymbol{l}\cdot\boldsymbol{s})^2\rangle = \frac{X}{4}, \tag{A3b}$$

$$\langle(\boldsymbol{l}\cdot\boldsymbol{s})^3\rangle = -\frac{X}{8}, \tag{A3c}$$

$$\langle(\boldsymbol{l}\cdot\boldsymbol{s})^4\rangle = \frac{X}{16}(X+1), \tag{A3d}$$

$$\langle(\boldsymbol{l}\cdot\boldsymbol{s})^5\rangle = -\frac{X}{32}(2X+1), \tag{A3e}$$

$$\langle(\boldsymbol{l}\cdot\boldsymbol{s})^6\rangle = \frac{X}{64}(X^2+3X+1), \tag{A3f}$$

$$\langle(\boldsymbol{l}\cdot\boldsymbol{s})^7\rangle = -\frac{X}{128}(X+1)(3X+1), \tag{A3g}$$

$$\langle(\boldsymbol{l}\cdot\boldsymbol{s})^8\rangle = \frac{X}{256}(X^3+6X^2+5X+1), \tag{A3h}$$

$$\langle(\boldsymbol{l}\cdot\boldsymbol{s})^9\rangle = -\frac{X}{512}(2X+1)(2X^2+4X+1), \tag{A3i}$$

$$\langle(\boldsymbol{l}\cdot\boldsymbol{s})^{10}\rangle = \frac{X}{1024}(X+1)(X^3+9X^2+6X+1), \tag{A3j}$$

where $X = l(l+1)$ is the square of the orbital angular momentum. A direct inspection of these equations shows that these average values obey the law

$$\langle(\boldsymbol{l}\cdot\boldsymbol{s})^k\rangle = \left(-\frac{1}{2}\right)^k X \sum_{j=0}^{\mathrm{Int}[k/2]-1} \binom{k-j-2}{j} X^j. \tag{A4}$$

## APPENDIX B: THIRD-ORDER MOMENTS INVOLVING SPIN-ORBIT AND ELECTRON-ELECTRON INTERACTION

Writing the interaction energy as a sum of electron-electron and spin-orbit parts $V_{\mathrm{int}} = V_{\mathrm{ee}} + V_{\mathrm{so}}$ the third-order moment in a $l^N$ configuration is written as

$$\langle(V_{\mathrm{int}} - \langle V_{\mathrm{int}}\rangle)^3\rangle = \mu^{(3)}_{\mathrm{ee}} + \mu^{(3)}_{\mathrm{ee\text{-}so}} + \mu^{(3)}_{\mathrm{so}}. \tag{B1}$$

The pure spin-orbit part $\mu^{(3)}_{\mathrm{so}}$ as been analyzed above [Eq. (12)]. The other contributions have been published previously by Kučas and Karazija [9]. Using standard second-quantization and angular-algebra techniques we could verify the expression for the crossed term,

$$\mu^{(3)}_{\mathrm{ee\text{-}so}} = \frac{3N(N-1)(4l+2-N)(4l+1-N)}{32l(2l+1)(4l-1)(4l+1)}\langle\xi\rangle^2 \times\left[\sum_k k(k+1)X_k - \frac{4l(l+1)(2l+1)}{4l+1}\sum_{k>0}X_k\right], \tag{B2a}$$

where $\langle\xi\rangle$ is the spin-orbit radial integral for the $nl$ orbital and $X_k$ is the product of the squared reduced matrix element $(l\|C^{(k)}\|l)^2$ and of the $F^{(k)}(ll)$ Slater integral [5],

$$X_k = (l\|C^{(k)}\|l)^2 F^{(k)}(ll) = (2l+1)^2\begin{pmatrix} l & k & l \\ 0 & 0 & 0\end{pmatrix}^2 F^{(k)}(ll). \tag{B2b}$$

We also performed some partial checks of Kučas and Karazija's formula for $\mu^{(3)}_{\mathrm{ee}}$. It turns out that the published formula contains a sign error. Therefore, we mention here the corrected expression

$$\begin{aligned}\mu^{(3)}_{\mathrm{ee}} = {}& \frac{N(N-1)(4l+2-N)(4l+1-N)}{(4l+2)(4l+1)4l(4l-1)(4l-2)(4l-3)}\sum_{\substack{k>0\\k'>0\\k''>0}}\Bigg\{[(4l-N)(4l-1-N)+(N-2)(N-3)] \\ &\times\left[\frac{3}{(2l+1)(4l+1)}\left(\frac{2\delta_{kk'}}{2k+1} - \begin{Bmatrix} l & l & k \\ l & l & k'\end{Bmatrix}\right) - \frac{2}{(2l+1)^2(4l+1)^2} + 2\begin{Bmatrix} k & k' & k'' \\ l & l & l\end{Bmatrix}^2 - \begin{Bmatrix} k & l & l \\ l & k' & l \\ l & l & k''\end{Bmatrix}\right] \\ &+2(N-2)(4l-N)\left[\frac{4\delta_{kk'}\delta_{k'k''}}{(2k+1)^2} - 6\frac{\delta_{kk'}}{2k+1}\begin{Bmatrix} l & l & k \\ l & l & k''\end{Bmatrix} + 3\begin{Bmatrix} l & l & k \\ l & l & k'\end{Bmatrix}\begin{Bmatrix} l & l & k \\ l & l & k''\end{Bmatrix}\right. \\ &\left.-2\begin{Bmatrix} k & k' & k'' \\ l & l & l\end{Bmatrix}^2 - \frac{6}{(2l+1)(4l+1)}\left(\frac{2\delta_{kk'}}{2k+1} - \begin{Bmatrix} l & l & k \\ l & l & k'\end{Bmatrix}\right) + \frac{4l+5}{(2l+1)^2(4l+1)^2}\right]\Bigg\}X_kX_{k'}X_{k''},\end{aligned} \tag{B3}$$

which has been successfully checked for $N = 2$ and 6, in an analytical or numerical way, respectively.

These formulas can be compared to Cowan's data presented in Sec. III A. From the above formulas and the values of the Slater integrals and the spin-orbit integral quoted there, we also get the centered third-order moments: 31677.1 $\mathrm{eV}^3$ for $V^3_{\mathrm{so}}$ only using Eq. (12); $-27817.6\ \mathrm{eV}^3$ for the $V_{\mathrm{ee}}V^2_{\mathrm{so}}$ contribution, Eq. (B2a); and 4251.4 $\mathrm{eV}^3$ for the $V^3_{\mathrm{ee}}$ contribution, Eq. (B3). The contribution for $V^3_{\mathrm{so}}$ and $V_{\mathrm{ee}}V^2_{\mathrm{so}}$ is therefore 3859 $\mathrm{eV}^3$, and the three-term sum is 8110.9 $\mathrm{eV}^3$. So we get a perfect agreement with both figures for the skewness in Table I, which are 8111 $\mathrm{eV}^3$ and $3.168\times10^4\ \mathrm{eV}^3$ according as electron interaction is accounted for or not. For highly charged ions the cross-term contribution, Eq. (B2a), is much simpler to evaluate than the $V^3_{\mathrm{ee}}$ contribution, Eq. (B3), and provides at least a qualitative estimate of the asymmetry. With the uncorrected asymmetry formula the $V^3_{\mathrm{ee}}$ contribution would have been 4545 $\mathrm{eV}^3$ and the three-term sum 8404 $\mathrm{eV}^3$, almost 300 $\mathrm{eV}^3$ away from Cowan's numerical data.

[1] C. Bauche-Arnoult, J. Bauche, and M. Klapisch, Phys. Rev. A **20**, 2424 (1979).
[2] C. Bauche-Arnoult, J. Bauche, and M. Klapisch, Phys. Rev. A **31**, 2248 (1985).
[3] S. A. Moszkowski, Progr. Theor. Phys. **28**, 1 (1962).
[4] E. Nardi and Z. Zinamon, Phys. Rev. A **20**, 1197 (1979).
[5] R. D. Cowan, *The Theory of Atomic Structure and Spectra* (University of California Press, Berkeley, California, 1981).
[6] J. Bauche, C. Bauche-Arnoult, and M. Klapisch, Adv. At. Mol. Phys. **23**, 131 (1988).
[7] J. Bauche, C. Bauche-Arnoult, and O. Peyrusse, *Atomic Properties in Hot Plasmas* (Springer Verlag, Berlin, 2015).
[8] R. Karazija, Acta Phys. Hung. **70**, 367 (1991).
[9] S. Kučas and R. Karazija, Phys. Scr. **47**, 754 (1993).
[10] P. H. M. Uylings, J. Phys. B: At. Mol. Opt. Phys. **17**, 2375 (1984).
[11] B. R. Judd, *Second Quantization and Atomic Spectroscopy* (John Hopkins Press, Baltimore, Maryland, 1967).
[12] A. Stuart and J. K. Ord, *Kendall's Advanced Theory of Statistics, Distribution Theory* (Charles Griffin and Co, London UK, 1987), Vol. 1.
[13] A. DasGupta, *Asymptotic Theory of Statistics and Probability* (Springer Verlag, New York, 2008).
[14] M. Abramowitz and I. Stegun, *Handbook of Mathematical Functions* (National Bureau of Standards, Washington DC, USA, 1972).
[15] J.-C. Pain and F. Gilleron, Phys. Rev. A **85**, 033409 (2012).
[16] F. Gilleron, J.-C. Pain, J. Bauche, and C. Bauche-Arnoult, Phys. Rev. E **77**, 026708 (2008).
[17] J.-C. Pain, F. Gilleron, J. Bauche, and C. Bauche-Arnoult, High Energy Density Phys. **5**, 294 (2009).